Catalysis Science & Technology

Accepted Manuscript

ROYAL SOCIETY OF CHEMISTRY

www.rsc.org/catalysis

Pd-Ag/SiO_2 bimetallic catalysts prepared by galvanic displacement for selective hydrogenation of acetylene in excess ethylene

Yunya Zhang, Weijian Diao, John R. Monnier, and Christopher T. Williams*

Department of Chemical Engineering, University of South Carolina, Swearingen Engineering Center, Columbia, SC 29208, USA. Email: willia84@cec.sc.edu; Tel: +1 (803) 777 0143; Fax: +1 (803) 777 8265

Abstract

A series of bimetallic Pd-Ag/SiO_2 catalysts were prepared by galvanic displacement with increasing loadings of Pd on Ag. The catalysts were characterized by atomic absorption spectroscopy, Fourier-transform infrared spectroscopy of CO adsorption and X-ray photoelectron spectroscopy. An actual Pd deposition beyond the theoretical limit for galvanic displacement suggested that the large difference in surface free energy for Pd and Ag resulted in Pd diffusion into the bulk of Ag particles, or Ag diffusion to the surface to provide fresh Ag atoms for further galvanic displacement. Characterization results indicated that on this series of catalysts the Pd atoms are distributed in very small ensembles or possibly even atomically on the Ag surface, and there was a transfer of electrons from Pd to Ag at all Pd loadings. For comparison, the catalysts were also evaluated for the selective hydrogenation of acetylene in excess ethylene at the conditions used in our previous study of the reverse Ag-Pd/SiO_2 catalysts. The selectivities for C_2H_4 formation remained high and constant due to the geometric effects that Pd atom existed as small ensembles. However, the electronic effects resulted in lower selectivities for C_2H_4 formation than those from the catalysts with high coverage of Ag on Pd.

Keywords: galvanic displacement; hydrogenation; acetylene; bimetallic catalysts; Pd-Ag.

1. Introduction

It has long been recognized that Pd provides superior performance on both activity and selectivity for the hydrogenation of acetylene to ethylene.[1,2] However, at high acetylene conversion the formation of ethane, C_4 and C_6 hydrocarbons is accelerated, which leads to the formation of carbonaceous residues that decrease the catalyst lifetime. To increase the selectivity to ethylene, Pd-based catalysts are usually modified with promoters, such as Ag, Ni, Cu, and K etc.[3-6] However, the bimetallic effects of the above additives are still not well understood, probably due to the conventional catalyst preparation methods that result in both monometallic and bimetallic particles with varying compositions. In our previous work[7], we used electroless deposition (ED)[8-12] to prepare a series of Ag- and Au-Pd/SiO_2 bimetallic catalysts with selective and controlled coverages of Ag and Au on Pd. The similar performance trends of enhanced selectivity of acetylene to ethylene at high coverages for Ag- and Au-Pd/SiO_2 suggested that the bimetallic effect for these catalysts was geometric and not electronic in nature. That is, at high coverages with smaller ensembles of Pd sites, acetylene is weakly adsorbed as a π-bonded species, which favors the hydrogenation to ethylene. On the other hand, acetylene is bonded in a multi-σ mode on larger ensembles of Pd and desorbs only as fully hydrogenated C_2H_6. Therefore, inspired by these previous results, the primary goal of this work was to prepare a series of reverse bimetallic catalysts (*i.e.* where Pd is deposited onto the Ag surface) in order to further explore the nature of bimetallic effects for the selective hydrogenation of acetylene.

For the synthesis of Pd-Ag bimetallic catalysts, galvanic displacement (GD) of Ag^0 by Pd^{2+} salts has been chosen. GD occurs when a base material is displaced by a metallic ion in solution that has a higher reduction potential than the displaced metal ion.[13-15] The base material is dissolved into the solution while the metallic ions in the solution are reduced on the surface of

the base material. This method is different from ED, in that GD does not require chemical reducing agents since the base metal itself already serves as the reducing agent. However, this redox reaction is usually limited by the accessibility of the base metal, resulting in passivation of the reaction when the entire surface of the base metal is covered.[14]

Over the past decade, GD has been widely used for the development of metal nanostructures with highly active surfaces for a variety of applications such as electrocatalysts[13,16-22], biomedicine[15], functional coatings[23,24], and deposition of metals on semiconductors[14,25]. Xia *et al.*[15,26-28] have thoroughly studied the mechanism of GD for tuning the properties of metal nanostructures through adjustment of composition, size, shape and morphology. Complex hollow nanostructures of Pd-Ir, Au-Ag, Pd-Ag, and Pt-Ag have been generated with potential for many applications. Yan *et al.*[13,20-22] also developed electrocatalysts with Pd-Au, Pt-Cu, Pt-Pd nanotubes or nanowires prepared by GD for the oxygen reduction and methanol oxidation reactions. Lee *et al.*[17-19] have investigated the performance of different forms of hollow and porous Pd-Ag or Pt-Ag nanomaterials prepared by GD as electrocatalysts for the oxygen reduction reaction. Maboudian and Carraro[14,23-25] have used GD to coat Au, Pt, Ag and Cu onto Si in thin film or nanoparticle forms for surface-enhanced Raman spectroscopy, and for improved interfacial behavior of semiconductors.

Although GD has been widely used in synthesizing electrocatalysts, it has had little application for the development of catalysts used in hydrogenation reactions. Sykes *et al.*[29] investigated the partial hydrogenation of phenylacetylene using PdCu alloy nanoparticles prepared by GD, which showed improvement in activity and selectivity compared to the corresponding monometallic catalysts. Li *et al.*[30] demonstrated that Pd/Co-B catalysts prepared by GD were extremely active and more selective than monometallic Pd and a Co-B amorphous

alloy for liquid-phase hydrogenation of 2-ethyl-2-hexenaldehyde to 2-ethyl-1-hexanol. Zhou *et al.*[31] used modified GD to prepare hollow Pt-Ni alloy nanospheres for liquid phase hydrogenation of p-chloronitrobenzene to p-chloroaniline. Such materials showed much higher activity, enhanced selectivity, and better durability than solid Pt nanoparticles.

In the present case, to be comparable with our previous work[7], SiO_2-supported Ag has been chosen as the base material for the preparation of various levels of Pd deposited by GD. From examination of standard reduction potentials, it is thermodynamically favorable for Pd^{2+} reduction to occur and to deposit on the Ag surface while Ag^0 is oxidized to Ag^+ ($Pd^{2+} + 2e^- = Pd^0$, $E° = 0.915V$; $Ag^+ + e^- = Ag^0$, $E° = 0.799V$). These bimetallic compositions have been characterized by Fourier-transform infrared (FTIR) spectroscopy of CO adsorption and X-ray photoelectron spectroscopy (XPS); catalysts have also been evaluated for the selective hydrogenation of acetylene in excess ethylene at the conditions used in our previous publication[7]. The results indicate that GD of Pd readily occurs but that catalyst surfaces are enriched in Ag due to diffusion of the Pd and/or the Ag components. Selectivity of acetylene hydrogenation is increased when small ensembles of Pd are located on the Ag surface.

2. Experimental

2.1. Catalyst preparation

The base material was 2.0 wt% Ag/SiO_2 prepared by incipient wetness using silver nitrate ($AgNO_3$, 99.9+%, Alfa Aesar) dissolved in de-ionized water and added to AEROSIL® OX 50 hydrophilic, fumed silica (Evonik Degussa Corporation) with a specific surface area of 50 ± 15 m^2/g. The fresh catalyst was then dried in a rotary evaporator at 60 °C under vacuum, and

calcined at 300 °C by flowing air for 2 h and reduced at 300 °C by flowing 10% H_2/He for 2 h in a horizontal furnace.

Controlled loadings of Pd were added to the silica-supported Ag surface by galvanic displacement. Briefly, palladium nitrate ($Pd(NO_3)_2$, 99.9%, Alfa Aesar) dissolved in 5% nitric acid (HNO_3, 68.0 – 70.0%, BDH) was used as the metal source of Pd^{2+}. Initial concentrations of the metal salts were selected based on the desired, theoretical coverage of Pd on Ag, assuming monolayer deposition and 1:1 surface stoichiometry of Pd on Ag. The volume of the galvanic displacement bath was 100 mL for each gram of the monometallic catalyst. The deposition of Pd was conducted at room temperature in disposable polyethylene beakers to prevent cross-contamination. The experiments were carried out with stirring on a magnetic stirring plate to ensure there were no external mass transfer limitations. A concentrated solution of nitric acid was added dropwise to the bath to maintain its pH at ~2.0 ± 0.1 during the entire experiment; a pH probe was immersed in the galvanic displacement bath to monitor the pH throughout the 1 h reaction time. Baths were prepared by adding all the required components except the monometallic Ag/SiO_2 catalyst. Addition of 1.0 g monometallic Ag/SiO_2 catalyst initiated the deposition. Liquid aliquots (≤ 1 mL) were periodically taken at different time intervals and filtered using 0.2 μm PTFE membrane syringe filters to remove catalyst particles. These liquid samples for monitoring the concentrations of Pd^{2+} remaining and Ag^{+} displaced in the bath were diluted separately by adding 10 vol% hydrochloric acid (HCl, 36.5 – 38.0%, BDH) and 0.5% lanthanum chloride ($LaCl_3$, 99.999%, Sigma-Aldrich) for Pd^{2+}, and 5 vol% HNO_3 for Ag^{+}, and then analyzed by atomic absorption spectroscopy(AAS, PerkinElmer AAnalyst 400). After 1 h of reaction time, the solution was filtered and the filtrate was washed thoroughly with 2 L of 18.2 MΩ-cm de-ionized water (Thermo Scientific Barnstead Nanopure Ultrapure Water System) to

remove all soluble salts. The catalyst was then dried *in vacuo* at room temperature and stored at ambient conditions. Thus, a complete series of Pd-Ag/SiO_2 bimetallic catalysts was prepared with varying weight loadings of Pd exchanged on the Ag surface.

2.2. Catalyst characterization

The concentration of Ag surface sites for the base 2 wt% Ag/SiO_2 catalyst was determined via chemisorption using hydrogen pulse titration of oxygen pre-covered Ag sites at 170 °C, as developed by Vannice[32]. Chemisorption was performed using a Micromeritics Autochem II 2920 automated chemisorption analyzer. The sample was reduced at 250 °C in 10% H_2/balance Ar for 2 h and then purged with pure Ar for 30 min, before cooling to 170 °C in flowing Ar. Next, 10% O_2/balance He was passed over the catalyst for 30 min at 170 °C to form Ag-O surface species before being purged with pure Ar for 30 min to remove residual, gas phase oxygen and oxygen weakly adsorbed on the support. Finally, 10% H_2/balance Ar was dosed at 170 °C until all surface Ag-O species reacted with hydrogen to form water and Ag^0 sites. For each Ag atom, a single H_2 molecule is consumed; hydrogen consumption was quantitatively measured using a high sensitivity thermal conductivity detector (TCD).

Fourier transfer infrared (FTIR) spectroscopy of CO adsorption was performed by using a Thermo Electron Nicolet Nexus 4700 spectrometer with a liquid nitrogen-cooled MCT-B (mercury-cadmium-telluride B) detector. Approximately 0.030 g catalyst was pressed into a self-supporting pellet with 12 mm diameter and then fixed in a sample holder that was placed in the middle of a temperature controlled, cylindrical flow cell. All samples were pretreated *in situ* at 200 °C in flowing 10% H_2/balance He for 2 h followed by flowing He for 30 min before cooling to room temperature in He. For each sample, a background spectrum in flowing He was first

taken and subtracted from all subsequent spectra. The sample was exposed to 1% CO/balance He for 30 min followed by a flow of pure He to remove any gas phase and reversibly-adsorbed CO. Spectra were collected continuously for 1 h in single beam absorbance mode with a resolution of 4 cm^{-1}. Spectra were baseline corrected and smoothed as needed to remove the noise due to water.

X-ray photoelectron spectroscopy (XPS) measurements were performed using a Kratos Axis Ultra DLD system with a hemispherical energy analyzer and a monochromatic Al Kα source operated at 15 keV and 150 W. The X-rays were incident at an angle of 45° with respect to the surface normal and the pass energy was fixed at 40 eV for the detailed scans. The powder samples were pressed into a cup of Mo stub and mounted in a catalysis cell that was attached to the XPS main chamber for *in situ* sample pretreatment. After the sample was reduced at 200 °C for 2 h, it was transferred into the UHV chamber for XPS analysis without exposure to air. A charge neutralizer was applied to compensate the residual positive charge present on the non-conductive silica support during photoemission. The Si 2p binding energy was used as a reference and was compared to the literature value of 103.3 eV. The same difference (charging correction) in eV was applied to all other XPS peaks to give corrected binding energy of Ag 3d and Pd 3d for both monometallic and bimetallic catalysts. For comparison, a reduced and commercially-available 2 wt% Pd/SiO_2 (BASF) was used as reference for the binding energy of Pd^0.

2.3. Catalyst evaluation

The monometallic Ag/SiO_2 and the series of bimetallic $Pd\text{-}Ag/SiO_2$ catalysts were evaluated for selective hydrogenation of acetylene in the presence of excess ethylene. Catalysts

were evaluated in a single pass, 0.19 in ID, packed bed, tubular reactor (316 stainless steel). The reactor was encased in a 1.0 in OD, jacketed shell with liquid inlet and exit ports at the bottom and top of the shell, respectively, which was connected to an ethylene glycol/H_2O recirculation bath to maintain isothermal behavior at 65 °C for this highly exothermic reaction. The reactor was wrapped with heating tape outside the jacket to heat the reactor to 200 °C when the catalyst was pretreated *in situ*. In all evaluations, the reactor was loaded with 0.050 g of catalyst to form a catalyst bed that was supported on glass wool in the middle of the reactor. A thermocouple was inserted into the catalyst bed to accurately monitor the reaction temperature and to ensure isothermal behavior. All catalysts were pretreated *in situ* at 200 °C in flowing 10% H_2/balance He for 2 h before being cooled to 65°C for evaluation.

All gas flows were maintained by mass flow controllers. To roughly approximate the tail-end feed of an ethylene cracker, the reaction feed stream for catalyst screening consisted of 1% C_2H_2, 20% C_2H_4, 5% H_2, balance He at a total flow rate of 50 SCCM corresponding to a GHSV value of 6.0×10^5 h^{-1}. Acetylene at 1% concentration was added from a pre-mixed cylinder of 10% C_2H_2/He by making the proper dilution. Both reaction feed and product streams were evaluated using an automated, on-line Hewlett-Packard 5890 Series II gas chromatograph using flame ionization detection. The feed and product analyses were typically made every 1.5 h. In addition to C_2H_2, C_2H_4, and C_2H_6, a number of C_4 hydrocarbons (n-butane, 1-butene, cis-2-butene, trans-2-butene, and 1,3-butadiene) were identified and quantitatively analyzed. These products can be considered as precursors to the "green oil" or C_2 oligomers commonly observed during industrial operation. All C_4 products were combined to give a total product and rates of formation that were normalized to C_2 feeds, *i.e.*, the molar quantities of C_4 products were multiplied by 2. All catalysts exhibited high, initial activities that underwent varying degrees of deactivation for the

approximately first 20 h on line. All the summary reaction data reported here were based on stable catalyst performance after 20 h on line to eliminate transient behavior. Similar deactivation trends have been observed by others and have been attributed to carbon-based fouling due to C_2H_2 oligomers on fresh catalyst surfaces.[1]

Conversion of C_2H_2 and selectivity of C_2H_2 to C_2H_4, C_2H_6 and C_4s were also defined in the same manner as our previous work[7] for consistency and comparison:

$$\text{Conversion of } C_2H_2 = \frac{C_2H_2 \text{ reacted}}{C_2H_2 \text{ (in)}}$$

$$\text{Selectivity of } C_2H_2 \text{ to } C_2H_4 = \frac{C_2H_2 \text{ reacted}}{C_2H_2 \text{ reacted} + C_2H_6 \text{ formed} + C_4\text{s formed} \times 2}$$

$$\text{Selectivity of } C_2H_2 \text{ to } C_2H_6 = \frac{C_2H_6 \text{ formed}}{C_2H_2 \text{ reacted} + C_2H_6 \text{ formed} + C_4\text{s formed} \times 2}$$

$$\text{Selectivity of } C_2H_2 \text{ to } C_4\text{s} = \frac{C_4\text{s formed} \times 2}{C_2H_2 \text{ reacted} + C_2H_6 \text{ formed} + C_4\text{s formed} \times 2}$$

$$C_2H_2 \text{ reacted} = C_2H_2 \text{ (in)} - C_2H_2 \text{ (out)}$$

$$C_2H_6 \text{ formed} = C_2H_6 \text{ (out)} - C_2H_6 \text{ (in)}$$

$$C_4\text{s formed} = \text{n-}C_4H_{10} \text{ (out)} + \text{t-2-}C_4H_8 \text{ (out)} + \text{1-}C_4H_8 \text{ (out)} + \text{c-2-}C_4H_8 \text{ (out)} + \text{1,3-}C_4H_6 \text{ (out)}$$

where (in) and (out) represent the feed stream and the product stream, respectively. This method of calculation cannot accurately be used for C_2H_4 hydrogenation, since C_2H_4 is a reaction product from selective C_2H_2 hydrogenation, and is also present in great excess as a feed component, making gas chromatographic analysis inaccurate.

3. Results and discussion

Silver dispersion and surface sites were measured for the base 2 wt% Ag/SiO_2 material prepared by incipient wetness. From chemisorption using H_2 titration of O-precovered Ag sites at 170 °C (H_2 titration uptake curves shown in Fig. S1 in Supplementary Information), the average Ag dispersion was 4.9%, which corresponds to an average Ag particle size of 23.8 nm and 5.52×10^{18} Ag surface sites per gram of catalyst, assuming spherical particle shape. This concentration of Ag surface sites was then used to calculate the theoretical coverage of Pd on Ag during GD. For further characterization, powder X-ray diffraction (XRD) on 2 wt% Ag/SiO_2 was performed and the profile was shown in Fig. S2 in Supplementary Information. The Ag particle size obtained from refinement of the XRD pattern was 19.6 nm, which is in good agreement with the chemisorption result.

The formation of true bimetallic Pd-Ag/SiO_2 catalysts prepared by GD requires that the Pd^{2+} cations should only react with Ag sites and not be adsorbed on the silica support. To prevent the unwanted strong electrostatic adsorption of Pd^{2+} cations onto silica, the pH of the galvanic displacement bath should be maintained below the point of zero charge (PZC) of the support where the SiO_2 surface is positively charged and cannot adsorb cations.[33,34] The PZC of the silica support used in this study was ~ pH 3.5, so the pH of the bath was maintained at 2.0 ± 0.1. The blank experiment with a bath of Pd^{2+} and silica support at pH 2 was conducted, and it can be seen (Fig. S3 in Supplementary Information) that there was no observed physisorption of Pd^{2+} on the silica support under this condition. On the other hand, at this condition it is thermodynamically favorable for Pd^{2+} reduction to occur by oxidation of Ag^0 to Ag^+. However, when the reaction was conducted in the pH 2 solution containing HNO_3, it was found that Ag^0 metal might be not only displaced by Pd^{2+} but also be oxidized by HNO_3. Thus, the dissolution

of Ag metal from 2 wt% Ag/SiO_2 in pH 2 HNO_3 solution was investigated prior to the GD experiments. From Fig. 1, it can be seen that the amount of Ag dissolution increased asymptotically with time to approximately 20 μmoles/g cat, or approximately 10% of the total Ag content dissolved within 1 h. The limiting value of 20 μmoles/g cat also suggests that only some of the Ag is susceptible to dissolution, such as those Ag atoms existing at corners and edges of 23.8 nm Ag particles. Therefore, to determine the concentration of displaced Ag^+ from 2 wt% Ag/SiO_2 due to GD, the amount of Ag^+ from HNO_3-facilitated Ag dissolution was subtracted from the total solution concentration of Ag^+. The remaining amount of Ag^+ was labeled as "corrected Ag^+" in figures and tables.

A series of bimetallic Pd-Ag/SiO_2 catalysts were prepared with increasing loadings of Pd on Ag. The time-dependent metal displacement profiles are illustrated in Fig. 2. Both the concentrations of deposited Pd^{2+} and corrected displaced Ag^+ were monitored during the experiments. For rigorous GD, the ratio of deposited Pd^{2+}/displaced Ag^+ is 1:2 for the reaction $Pd^{2+} + 2Ag^0 \rightarrow Pd^0 + 2Ag^+$. The Pd coverage should then be limited to 0.5 monolayers on Ag, since two Ag surface atoms are required for each Pd^{2+} deposited. However, the 0.03, 0.09, 0.28, and 0.32 wt% Pd-Ag samples shown in Fig. 2A correspond to 0.3, 0.9, 2.9, and 3.3 theoretical monolayers coverage on Ag, when Ag dissolution is not taken into account. The analyzed compositions of the catalysts are summarized in Table 1 and indicate that for the higher Pd loadings substantial loss of Ag has occurred, primarily by galvanic displacement (dissolution of Ag^+ in the acidic solution is less important for the higher Pd loadings). For the samples designated as 0.39 and 0.44 wt% Pd, the molar ratios of [Ag]/[Pd] are only about 2.5, corresponding to a bulk empirical formula of $Ag_{0.7}Pd_{0.3}$. Thus, extensive mixing of Ag and Pd in the bimetallic particles has occurred.

The increased Pd deposition beyond the theoretical limit for GD indicates one of two possibilities. First, there were perhaps defects on the Ag surface that permitted access of Pd^{2+} to more Ag metal sites in the sub-surface region. Alternatively, there was diffusion of Pd into the bulk of Ag particles, or more likely, migration of Ag to the surface. Indeed, the surface free energy of Ag metal is lower than that of Pd metal based on calculated and experimental results from others.[35-38] Mezey[37] reported surface free energies (SFE) of 2043 and 1302 ergs/cm^2 for Pd and Ag metallic surfaces at 298 K, respectively, indicating that it is thermodynamically preferred for Ag to diffuse to the surface of a Ag-Pd bimetallic particle. Tang[38] has also calculated the SFE values of specific Ag facets and estimated the free energies of the two most common facets of Ag particles, the (111) and (100) surfaces, are 881 and 948 ergs/cm^2, further showing the thermodynamic favorability for Ag diffusion to the surface of Pd-Ag bimetallic particles. In support of the first possibility, Xia *et al.*[39] reported that when Na_2PdCl_4 was added to a suspension of Ag nanocubes, etch pits developed on the surfaces of the nanocubes, primarily at the corners. Oxidation within the etch pits removed Ag (as Ag^+) from the interior rather than the surface of the nanocubes to simultaneously reduce Pd on the exterior of the Ag nanocubes. Although the supported Ag particles in this study likely exist as spherical particles, there are still corners and edges that might provide etch pits for access to the interior of the Ag particles. However, the more likely explanation is that the large difference in SFE values for Ag and Pd result in Ag diffusion to the surface to provide fresh Ag atoms for galvanic displacement with Pd^{2+}.

It can be seen in Fig. 2A that the displacement reaction is initially first order in Pd^{2+}, but as the Ag surface becomes depleted the rate of displacement decreases. Explicit plots of first order reaction for Pd^{2+} disappearance vs. time for 0.09 – 0.32 wt% Pd-Ag samples are shown in

Fig. S4 in Supplementary Information. Fig. 2B shows, as mentioned earlier, the concentration of corrected Ag^+, which is the actual amount of the galvanically-displaced Ag^+. The decrease in Pd^{2+} and increase in corrected Ag^+ in the solution confirm that GD does occur. For the 0.32 wt% Pd-Ag sample the reaction was conducted with a much higher initial concentration of Pd^{2+} in an attempt to achieve more deposition. However, Pd^{2+} deposition ceased after around 30 min, leaving more than 20 μmoles Pd^{2+}/g cat in solution to give a similar amount of deposition as the 0.28 wt% Pd-Ag sample, indicating that galvanic displacement has reached an upper limit and is not kinetically dependent on the concentration of Pd^{2+} remaining in solution. To determine whether higher temperatures increased displacement, bath temperatures of 50 and 75 °C were examined and the corresponding kinetic curves of deposited Pd^{2+} and displaced Ag^+ are shown in Fig. 3A and Fig. 3B, respectively. The results shows that galvanic displacement increased at higher temperatures, suggesting that activated diffusion of Ag to the surface occurred during GD, again due to differences in the surface free energies of Ag and Pd.

To determine the concentrations of surface Pd on Ag, the standard H_2-O_2 titration at 40 °C used for Pd metal[7,8] (see procedures in Supplementary Information) was conducted for all samples. Titration pulse curves of H_2 for all samples are shown in Fig. S5. For the highest Pd weight loading sample (0.44 wt% Pd-Ag), 2.49×10^{19} Pd atoms/g cat were deposited on the Ag surface. However, there was no significant H_2 uptake for this sample as well as for all other samples, suggesting that the surface was highly enriched with Ag. This is inconsistent with the observation that during the preparation of samples with high Pd weight loadings, the GD reaction stopped suggesting there were no exposed Ag atoms. Such contradictory results might be caused by the pretreatment step during the chemisorption. The 2 h reduction at 200 °C for Pd-Ag samples may cause Ag atoms with lower surface energy to move from the bulk to the surface or

possibly drive Pd atoms with higher surface energy into the subsurface of Ag. The effects are the same; Ag becomes enriched at the surface of the bimetallic particle. The Pd-Ag system is a well-known binary alloy[40] and such migration of Pd into the bulk and/or Ag moving to the surface may result in the formation of a Pd-Ag alloy near the catalyst surface.

To explore further the distribution of Pd atoms on the Ag surface, FTIR spectroscopy of CO adsorption at room temperature was conducted on the *in situ* reduced, monometallic Ag/SiO_2 and bimetallic $Pd\text{-}Ag/SiO_2$ catalysts. Representative spectra for the different Pd loadings are shown in Fig. 4. There were no CO vibrations observed for Ag/SiO_2 sample, which is in agreement with the observations of Rodriguez *et al.*[41] that Ag^0 is inactive for CO adsorption. The FTIR spectra of the CO adsorption on the commercial 1.85 wt% Pd/SiO_2 catalyst was previously published by our group.[12] For $Pd\text{-}Ag/SiO_2$ samples, a single CO stretching band was observed in the 2000-2100 cm^{-1} region with the peak centered at approximately 2046 cm^{-1}, which was attributed to linearly adsorbed CO on fully reduced Pd sites[12,42,43]. However, bridge-bond CO between 1800-2000 cm^{-1} was not observed. This result indicates that some surface Pd is present and that the Pd atoms are distributed in very small ensembles, possibly even atomically, on the Ag surface. The scarcity of Pd sites may also indicate that the 200 °C reduction treatment contributes to a Ag-rich surface, either by diffusion of Pd to into the bulk or migration of the Ag to the surface, to leave only a scattered distribution of Pd atoms on the surface. However, the much lower value of SFE for Ag suggests that subsurface Ag atoms migrate to the surface, covering the Pd atoms to give a Ag-enriched bimetallic surface. The peak intensity increases gradually with increasing Pd weight loadings, indicating that the bulk particles become more saturated with Pd atoms at higher weight loadings and that more Pd atoms remain exposed on the surface. It is also possible that exposure to CO for the FTIR experiments may cause Pd atoms to

migrate to the surface of the catalyst due to the high heat of adsorption for CO on Pd[44]; however, the Pd-catalyzed activity of these compositions for C_2H_2 hydrogenation (later point in this manuscript) suggest the surface Pd sites were initially present, but too low for accurate chemisorption.

In addition to changes in peak intensity, shifts in vibrational band positions were observed with addition of Pd to Ag. Typically, CO coverages increase with more Pd on the surface, which results in greater CO dipole-dipole interactions and an accompanying shift to higher frequencies.[42] Conversely, in the present case (Fig. 4) peaks for CO adsorption shift to lower frequencies as the Pd weight loadings increased. This is consistent with what was observed in a previous study from our group[12] for Ag-Pd/SiO_2 prepared by ED of Ag on Pd. In that case, the CO adsorption peaks shifted to higher frequencies as the deposited Ag diluted the Pd surface into smaller ensembles. It was proposed that the frequency shift was related to an electronic effect between Pd and Ag. XPS analyses showed the Ag $3d_{5/2}$ binding energy (BE) was shifted to lower values when deposited on Pd; as the surface coverage of Ag on Pd increased, the BE shift decreased from 0.7 to 0.1. The BE shifts decreased with coverage because the higher surface coverages of Ag resulted in autocatalytic deposition to form three dimensional aggregates of Ag that were more similar to bulk Ag metal particles. The BE shift was maximized at the lowest level of deposition since the Ag was essentially distributed in a monodisperse manner on the Pd surface to give the maximum e^- transfer from Pd to Ag. The direction of the CO stretching frequency shift suggested that the decrease of the electron density of surface Pd atoms lowered the back donation from non-bonding electrons of Pd to the π^* orbitals of CO. This electronic interaction appeared to outweigh any shift to lower frequencies due to lower dipole-dipole interactions.

In the present study, e^- transfer from Pd to Ag should be maximized for the lowest levels of galvanically-exchanged Pd since the number of Pd-Ag interactions (e^- transfer from Pd to Ag) is highest at these conditions. For the 0.09 wt% Pd sample, the empirical formula of the bimetallic particles corresponds to $Ag_{0.94}Pd_{0.06}$ to give a very dilute Pd composition, which should exhibit the greatest extent of Pd-Ag interaction. This results in less electron donation from non-bonding electrons of Pd to the π* orbitals of CO to give a higher C-O bond order and an upshifted C-O stretching frequency.

To examine the surface/near-surface of the Pd-Ag samples, XPS measurements were performed with detailed scans of the Pd 3d and Ag 3d orbitals, and the binding energies were compared with the values obtained from the monometallic (reference) catalysts. The Si 2p peak of the support was used as an internal standard to confirm the peak positions, and all peak intensities for Pd 3d and Ag 3d were normalized to Si 2p peak intensity for comparison. Results shown in Fig. 5A confirm there was Pd at least in the near surface (escape depth of photoelectrons is several lattice layers) of the catalysts prepared by galvanic displacement. The Pd and Ag peak intensities in Fig. 5A and Fig. 5B also indicate, as expected, that near surface Pd concentrations increase and Ag concentrations decrease when more Pd metal is galvanically-exchanged.

The assignment of Ag oxidation state by XPS is a matter of controversy. A large discrepancy and superposition of binding energy values of Ag 3d exists in the literatures[45-51]: Ag $3d_{5/2}$ is reported to be from 366.4 to 369.2 eV for Ag^0; from 367.5 to 368.8 eV for Ag_2O; and from 367.4 to 368.4 eV for AgO. Therefore, some studies[45-47] report a negative shift for oxidized $Ag^{\delta+}$ versus Ag^0, while others[48-51] observe a positive shift instead. Because of the uncertainty of Ag 3d binding energies of supported Ag catalysts, presumably due to the charging effects of the

insulating silica support and possible Ag particle size effects, comparisons of Ag binding energies are valid only within a given study for similar Ag morphologies and particle size. To confirm the Ag $3d_{5/2}$ binding energies for Ag^0 and Ag^+ (or $Ag^{\delta+}$) species in this study, the XPS spectra for 2 wt% Ag/SiO_2 (Fig. S6 in Supplementary Information) were taken after reduction in 100% H_2 at 200 °C for 2 h and after calcination in 100% O_2 at 200 °C for 2 h. The Ag $3d_{5/2}$ values are 367.9 eV after reduction and 368.7 eV after calcination, corresponding to Ag^0 and Ag^+ respectively. Thus, the shift to higher Ag $3d_{5/2}$ binding energy value in this study indicates electron transfer away from Ag. The similar trend on 12 wt% Ag/Al_2O_3 sample was observed in a previous study from our group.[51] However, because of the complexity and controversy of binding energy shift for Ag systems, other reasonable explanations[48-50] for a positive shift due to factors other than an oxidation state change in Ag cannot be ruled out. For all bimetallic compositions in this study, shifts to higher binding energies were observed for the Pd $3d_{3/2}$ and Pd $3d_{5/2}$ peaks in comparison to 2 wt% Pd/SiO_2 catalyst. Conversely, the Ag $3d_{3/2}$ and Ag $3d_{5/2}$ peaks were shifted to lower binding energies compared to a 2 wt% Ag/SiO_2 catalyst. These shifts of Pd 3d and Ag 3d peaks indicate a net electron transfer from Pd to Ag, which is also consistent with previous work from our group[12] for Ag-Pd/SiO_2 catalysts prepared by ED of Ag on Pd.

As more Pd is deposited onto Ag, the binding energy shift to lower values for Ag in Fig. 5B increases from 0.4 eV for 0.09 wt% Pd to 0.6 eV for 0.39 wt% Pd since there are more Pd atoms to interact with neighboring Ag atoms. Because Ag is the majority component in these bimetallic particles, the magnitude of the BE shift is somewhat dampened by those Ag atoms that do not interact with Pd atoms. Higher Pd loadings increase the number of Pd-Ag interactions. The upshift in Pd $3d_{5/2}$ BE values is approximately 0.4 eV for all Pd loadings since all Pd atoms are interactive with neighboring Ag atoms. The observed binding energy shifts for the Pd-Ag

bimetallic catalysts as a function of Pd weight loading are consistent with the red shift of the CO-Pd vibrational band observed by FTIR spectroscopy and lend further credence to the supposition that there was a transfer of electrons from Pd to Ag.

Selective hydrogenation of acetylene in the presence of excess ethylene was carried out for the different compositions of Pd-Ag/SiO_2 catalysts at the same reaction conditions used for the Ag-Pd/SiO_2 bimetallic catalysts reported in our previous work[7]. The exception was that increased weights of catalysts were required to account for the lower number of accessible Pd sites with these catalysts.

Fig. 6A shows conversion of acetylene and selectivity of acetylene hydrogenation towards ethylene as a function of Pd weight loading on Ag/SiO_2. No data are shown for 0.09 wt% Pd-Ag/SiO_2 because activity was too low for accurate measurement. The base Ag/SiO_2 catalyst exhibited no reactivity for acetylene hydrogenation during a control experiment. The C_2H_2 conversion increased from 2.0% to 17.5% with increasing Pd weight loadings, consistent with the FTIR results that showed more Pd on the Ag surface for higher levels of Pd deposited by GD. Selectivities for C_2H_4 formation remained essentially constant at approximately 80% for the different Pd loadings; likewise, the selectivities for C_2H_6 and C_4 hydrocarbons were also relatively constant for the different Pd loadings (Fig. 6B). This indicates that the ensemble sizes and electronic charges of Pd sites were similar over this composition range, since changes in Pd ensemble sizes and/or changes in electronic charges of the Pd surface sites would be expected to change the selectivity for C_2H_4 formation[52]. Atomic, or near atomic dispersion of surface Pd sites should favor π-bonded C_2H_2 which favors C_2H_4 formation.[7] Since FTIR and XPS analyses indicated that the Pd ensemble sizes and electronic Pd 3d states were constant over this range of Pd weight loadings, catalyst selectivities should also remain the same.

In our previous work for the electroless deposition of Ag and Au on Pd catalysts, C_2H_2 conversions decreased with increasing Group IB coverage (fewer surface Pd atoms were exposed).[7] However, selectivity of C_2H_2 to C_2H_4 was enhanced at higher Ag and Au coverages, particularly for fractional coverages high than 0.80. The similar performance trends for both Ag-Pd and Au-Pd catalysts suggested the bimetallic effect was primarily geometric and not electronic in nature. That is, at high Group IB coverages with smaller ensembles of contiguous Pd sites, acetylene was weakly adsorbed as a π-bonded species, which favored the hydrogenation to ethylene which readily desorbed. On the other hand, acetylene was bonded in a multi-σ mode on larger ensembles of Pd and desorbed only when fully hydrogenated to C_2H_6. However, the selectivity values for C_2H_4 formation at high coverages of Ag and Au for the Ag-Pd and Au-Pd catalysts were as high as 86 – 90%, which is noticeably greater than 80% for this family of catalysts. Recent computational studies by Neurock[52] and Nørskov[53] for acetylene hydrogenation on Ag(111), Pd(111), $Pd_{0.75}Ag_{0.25}$/Pd(111), and $Pd_{0.50}Ag_{0.50}$/Pd(111) have shown that while the geometric effects of Pd surface dilution into small Pd ensembles by Ag are more important than electronic effects of Ag on Pd atoms, there are still observable electronic effects. Any electronic effect that lowers the adsorption energy of C_2H_2 will increase selectivity of hydrogenation to form C_2H_4. Our XPS and FTIR data show e^- transfer from Pd to Ag, leaving the Pd surface sites somewhat e^- deficient. This results in stronger interaction between Pd and the e^- rich π-bond system of C_2H_2 to give higher adsorption energies of π-bonded C_2H_2. This higher adsorption energy increases the extent of hydrogenation of C_2H_2 to C_2H_6 before desorption can occur. This is more pronounced in our current study because Pd is the minority component and more susceptible for e^- transfer to Ag; Table 1 confirms the minority compositions of the different bimetallic catalysts. In our earlier study[7] where Ag was confined to only the surface, Pd was by

far the majority component with more limited Pd-Ag electronic interactions; hence the somewhat higher selectivities for C_2H_2 hydrogenation to C_2H_4.

4. Conclusions

A series of bimetallic Pd-Ag/SiO_2 catalysts were prepared by galvanic displacement with increasing loadings of Pd on Ag. The actually increased Pd deposition beyond the theoretical limit for galvanic displacement indicated that the large difference in surface free energy for Pd and Ag resulted in Pd diffusion into the bulk of Ag particles, or Ag diffusion to the surface to provide fresh Ag atoms for further galvanic displacement. Such migration led to the formation of a Pd-Ag alloy near the catalyst surface. FTIR results revealed that the Pd atoms on all prepared catalysts are distributed in very small ensembles or possibly even atomically on the Ag surface. Such geometric effects were further confirmed by evaluation studies revealing that the selectivities for C_2H_4 formation remained high and constant for different Pd loadings. However, unlike for the case of Ag on Pd surfaces[7], the Pd sites here are significantly influenced by the electron transfer from Pd to Ag. This results in a competing electronic effect in these catalysts that limits the ability to obtain very high selectivity towards C_2H_4.

Acknowledgement

The authors gratefully acknowledge NSF No. 0854339 for funding a portion of this work and are appreciative to Dr. Shuguo Ma and Dr. Ye Lin for their expert XPS analysis.

References

1 G. C. Bond, D. A. Dowden, and N. Mackenzie, *Trans. Faraday. Soc.*, 1958, **54**, 1537-1546.

2 A. Borodziński, and G. C. Bond, *Catal. Rev.: Sci. Eng.*, 2006, **48**, 91-144.

3 D. C. Huang, K. H. Chang, W. F. Pong, P. K. Tseng, K. J. Hung, and W. F. Huang, *Catal. Lett.*, 1998, **53**, 155–159.

4 P. Miegge, J. L. Rousset, B. Tardy, J. Massardier, and J. C. Bertolini, *J. Catal.*, 1994, **149**, 404-413.

5 S. Leviness, V. Nair, and A. H. Weiss, *J. Mol. Catal.*, 1984, **25**, 131-140.

6 V. H. Sandoval, and C. E. Gigola, *Appl. Catal., A*, 1996, **148**, 81-96.

7 Y. Zhang, W. Diao, C. T. Williams, and J. R. Monnier, *Appl. Catal., A*, 2014, **469**, 419-426.

8 M. T. Schaal, A. Y. Metcalf, J. H. Montoya, J. P. Wilkinson, C. C. Stork, C. T. Williams, and J. R. Monnier, *Catal. Today*, 2007, **123**, 142-150.

9 M. T. Schaal, A. C. Pickerell, C. T. Williams, and J. R. Monnier, *J. Catal.*, 2008, **254**, 131-143.

10 K. D. Beard, J. W. Van Zee, and J. R. Monnier, *Appl. Catal., B*, 2009, **88**, 185-193.

11 M. T. Schaal, J. Rebelli, H. M. McKerrow, C. T. Williams, and J. R. Monnier, *Appl. Catal., A*, 2010, **382**, 49-57.

12 J. Rebelli, A. A. Rodriguez, S. Ma, C. T. Williams, and J. R. Monnier, *Catal. Today*, 2011, **160**, 170-178.

13 S. M. Alia, Y. S. Yan, and B. S. Pivovar, *Catal. Sci. Technol.*, 2014, **4**, 3589-3600.

14 C. Carraro, R. Maboudian, and L. Magagnin, *Surf. Sci. Rep.*, 2007, **62**, 499-525.

15 X. Xia, Y. Wang , A. Ruditskiy, and Y. Xia, *Adv. Mater.*, 2013, **25**, 6313-6333.

16 L. Jiang, A. Hsu, D. Chu, and R. Chen, *Electrochim. Acta*, 2010, **55**, 4506-4511.

17 C. -L, Lee, and C. -M, Tseng, *J. Phys. Chem. C*, 2008, **112**, 13342-13345.

18 C. -L, Lee, C. -M, Tseng, R. -B Wu, C. -C, Wu, and S. -C, Syu, *Electrochim. Acta*, 2009, **54**, 5544-5547.

19 C. -W, Chen, Y. -S, Hsieh, C. -C, Syu, H. -R, Chen, and C. -L, Lee, *J. Alloys Compd.*, 2013, **580**, S359-S363.

20 S. M. Alia, K. Duong, T. Liu, K. O. Jensen, and Y. Yan, *ChemSusChem*, 2014, **7**, 1739-1744.

21 S. M. Alia, B. S. Pivovar, and Y. Yan, *J. Am. Chem. Soc.*, 2013, **135**, 13473-13478.

22 S. M. Alia, K. O. Jensen, B. S. Pivovar, and Y. Yan, *ACS Catal.*, 2012, **2**, 858-863.

23 A. Gutés, R. Maboudian, and C. Carraro, *Langmuir*, 2012, **28**, 17846-17850.

24 A. Gutes, I. Laboriante, C. Carraro, and R. Maboudian, *J. Phys. Chem. C*, 2009, **113**, 16939-16944.

25 L. Magagnin, R. Maboudian, and C. Carraro, *J. Phys. Chem. B*, 2002, **106**, 401-407.

26 L. Au, X. Lu, and Y. Xia, *Adv. Mater.*, 2008, **20**, 2517-2522.

27 M. Liu, Y. Zheng, S. Xie, N. Li, N. Lu, J. Wang, M. J. Kim, L. Guo, and Y. Xia, *Phys. Chem. Chem. Phys.*, 2013, **15**, 11822-11829.

28 H. Zhang, M. Jin, H. Liu, J. Wang, M. J. Kim, D. Yang, Z. Xie, J. Liu, and Y. Xia, *ACS Nano*, 2011, **5**, 8212-8222.

29 M. B. Boucher, B. Zugic, G. Cladaras, J. Kammert, M. D. Marcinkowski, T. J. Lawton, E. C. H. Sykes, and M. Flytzani-Stephanopoulos, *Phys. Chem. Chem. Phys.*, 2013, **15**, 12187-12196.

30 J. Ma, L. Xu, L. Xu, H. Wang, S. Xu, H. Li, S. Xie, and H. Li, *ACS Catal.*, 2013, **3**, 985-992.

31 H. Li, H. Lin, Y. Hu, H. Li, P. Li, and X. Zhou, *J. Mater. Chem.*, 2011, **21**, 18447-18453.

32 S. R. Seyedmonir, D. E. Strohmayer, G. L. Geoffroy, M. A. Vannice, H. W. Young, and J. W. Linowski, *J. Catal.*, 1984, **87**, 424-436.

33 J. P. Brunelle, *Pure Appl. Chem.*, 1978, **50**, 1211-1229.

34 J. R. Regalbuto in *Catalyst Preparation: Science and Engineering*, ed. J. R. Regalbuto, CRC Press, Boca Raton, 2006, ch. 13, pp. 297-318.

35 W. R. Tyson, and W. A. Miller, *Surf. Sci.*, 1977, **62**, 267-276.

36 H. L. Skriver, and N. M. Rosengaard, *Phys. Rev. B*, 1992, **46**, 7157-7168.

37 L. Z. Mezey, and J. Giber, *Jpn. J. Appl. Phys.*, 1982, **21**, 1569-1571.

38 J. Tang, L. Deng, H. Deng, S. Xiao, X. Zhang, and W. Hu, *J. Phys. Chem. C*, 2014, **118**, 27850-27860.

39 J. Chen, B. Wiley, J. McLellan, Y. Xiong, Z. -Y. Li, and Y. Xia, *Nano Lett.*, 2005, **5**, 2058-2062.

40 H. Okamoto, in *Desk Handbook: Phase Diagrams for Binary Alloys*, ASM International, Materials Park, Ohio, 2nd edn., 2010, pp. 2-24.

41 J. A. Rodriguez, C. M. Truong, and D. W. Goodman, *Surf. Sci.*, 1992, **271**, L331-L337.

42 P. Gelin, A. R. Siedle, and J. T. Yates Jr., *J. Phys. Chem.*, 1984, **88**, 2978-2985.

43 J. B. Giorgi, T. Schroeder, M. Bäumer, and H. -J. Freund, *Surf. Sci.*, 2002, **498**, L71–L77.

44 D. Childers, A. Saha, N. Schweitzer, R. M. Rioux, J. T. Miller, *ACS Catal.*, 2013, **3**, 2487-2496.

45 Z. Qu, G. Ke, Y. Wang, M. Liu, T. Jiang, J. Gao, *Appl. Surf. Sci.*, 2013, **277**, 293-301.

46 M. Skaf, S. Aouad, S. Hany, R. Cousin, E. Abi-Aad, A. Aboukaïs, *J. Catal.*, 2014, **320**, 137-146.

47 V. I. Pârvulescu, B. Cojocaru, V. Pârvulescu, R. Richards, Z. Li, C. Cadigan, P. Granger, P. Miquel, C. Hardacre, *J. Catal.*, 2010, **272**, 92-100.

48 A. M. Venezia, L. F. Liotta, G. Deganello, Z. Schay, D. Horváth, L. Guczi, *Appl. Catal., A*, 2001, **211**, 167-174.

49 M. Al-Hada, S. Peters, S. Peredkov, M. Neeb, W. Eberhardt, *Surf. Sci.*, 2015, **639**, 43-47.

50 A. M. Ferraria, A. P. Carapeto, A. M. Botelho do Rego, *Vacuum*, 2012, **86**, 1988-1991.

51 W. Diao, C. D. DiGiulio, M. T. Schaal, S. Ma, J. R. Monnier, *J. Catal.*, 2015, **322**, 14-23.

52 D. Mei, M. Neurock, and C. M. Smith, *J. Catal.*, 2009, **268**, 181-195.

53 F. Studt, F. Abild-Pederson, T. Bligaard, R. Z. Sørenson, C. H. Christenson, and J. K. Nørskov, *Angew. Chem. Int. Ed.*, 2008, **47**, 9299-9302.

Table Captions

Table 1 Composition of Pd-Ag catalysts after galvanic displacement experiments. Actual catalyst compositions based on analyzed Ag and Pd loadings, not predictive stoichiometries

Figure Captions

Fig. 1 Ag dissolution from 2 wt% Ag/SiO_2 in pH 2 HNO_3 solution at room temperature.

Fig. 2 Time-dependent galvanic displacement profiles of (A) deposited Pd^{2+} from bath solution and (B) galvanically displaced Ag^+ from 2 wt% Ag/SiO_2 at room temperature with different initial Pd^{2+} concentrations.

Fig. 3 Time-dependent galvanic displacement profiles of (A) deposited Pd^{2+} from bath solution and (B) galvanically displaced Ag^+ from 2 wt% Ag/SiO_2 at 25, 50 and 75 °C with same initial Pd^{2+} concentration.

Fig. 4 FTIR spectra for CO adsorption on various Pd-Ag/SiO_2 bimetallic catalysts.

Fig. 5 XPS spectra of (A) Pd 3d on 2 wt% Pd/SiO_2 and Pd-Ag/SiO_2 and (B) Ag 3d on 2 wt% Ag/SiO_2 and Pd-Ag/SiO_2. All samples were reduced *in situ* at 200 °C in 100% H_2 for 2 h.

Fig. 6 (A) Conversion of acetylene and selectivity of acetylene to ethylene and (B) selectivity of acetylene to ethane and C_4s as a function of Pd weight loadings on Ag/SiO_2. Reaction conditions: 65°C and feed composition of 1% C_2H_2, 5% H_2, 20% C_2H_4, and balance He at GHSV = 6.0×10^5 h^{-1}. Error bars represent maximum and minimum values for each data point; data point is average value.

Table 1 Composition of Pd-Ag catalysts after galvanic displacement experiments. Actual catalyst compositions based on analyzed Ag and Pd loadings, not predictive stoichiometries

Catalyst Designation	Initial Ag loading, (%)	Final Ag loading after dissolution and GD, (%)	Ag loss based on AA analysis, (%)	Actual metal composition of catalyst	Molar ratio of Ag to Pd
2 wt% Ag/SiO_2	2.0	—	—	2 wt% Ag	—
0.03 wt% Pd	2.0	1.71	14.5	0.03 wt% Pd - 1.71 wt% Ag	56.2
0.09 wt% Pd	2.0	1.50	25.0	0.09 wt% Pd - 1.50 wt% Ag	16.4
0.28 wt% Pd	2.0	1.42	29.0	0.28 wt% Pd - 1.43 wt% Ag	5.0
0.32 wt% Pd	2.0	1.21	39.5	0.32 wt% Pd - 1.21 wt% Ag	3.7
0.39 wt% Pd	2.0	1.01	49.5	0.39 wt% Pd - 1.01 wt% Ag	2.6
0.44 wt% Pd	2.0	1.02	49.0	0.44 wt% Pd - 1.02 wt% Ag	2.3

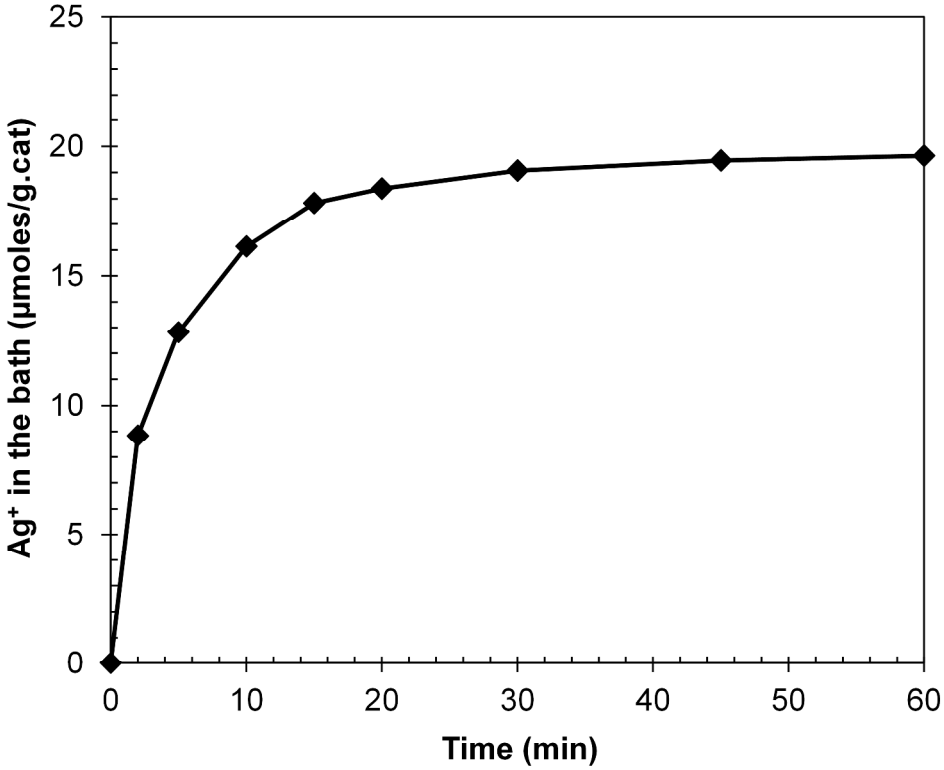

Fig. 1 Ag dissolution from 2 wt% Ag/SiO_2 in pH 2 HNO_3 solution at room temperature.

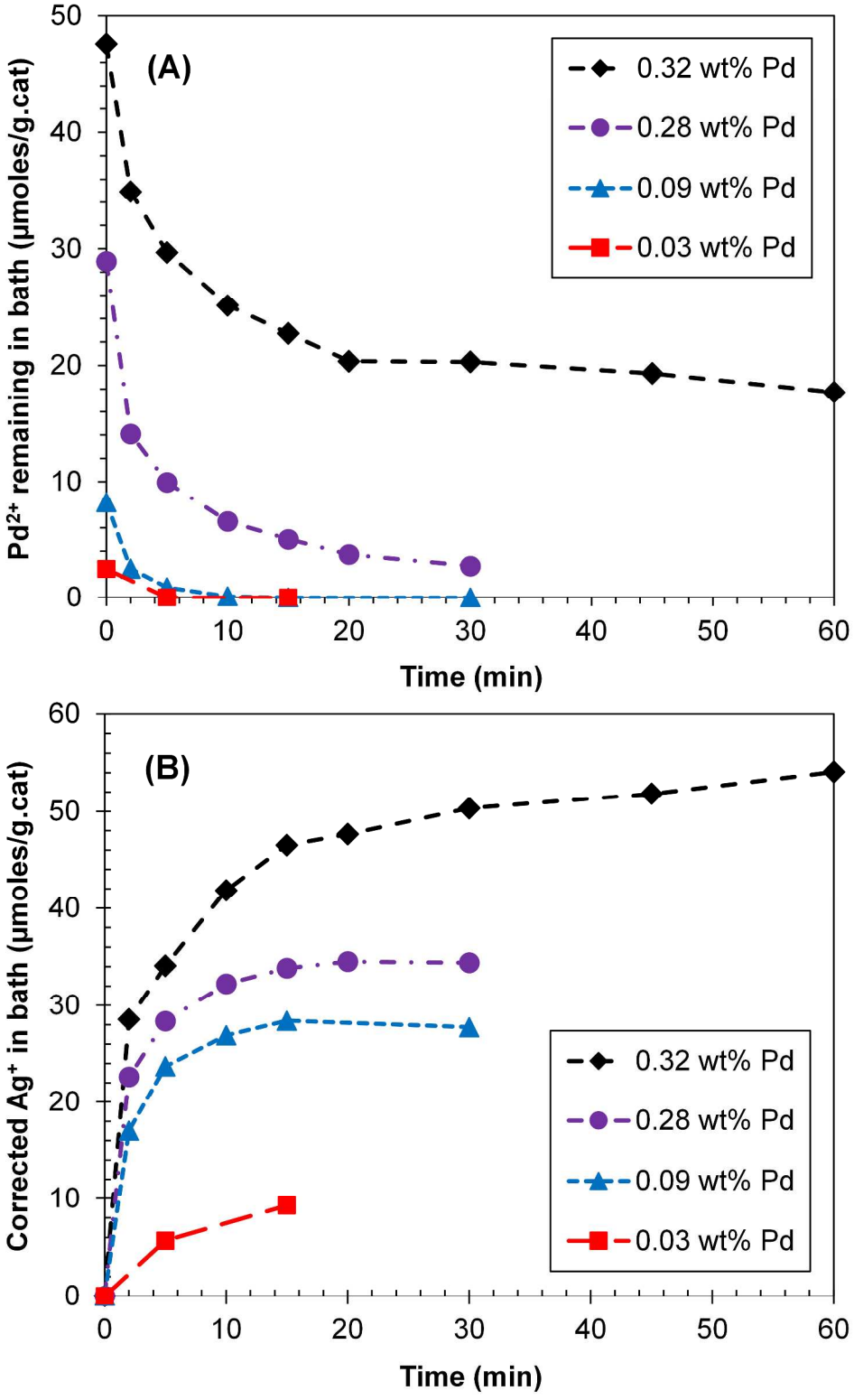

Fig. 2 Time-dependent galvanic displacement profiles of (A) deposited Pd^{2+} from bath solution and (B) galvanically displaced Ag^{+} from 2 wt% Ag/SiO_2 at room temperature with different initial Pd^{2+} concentrations.

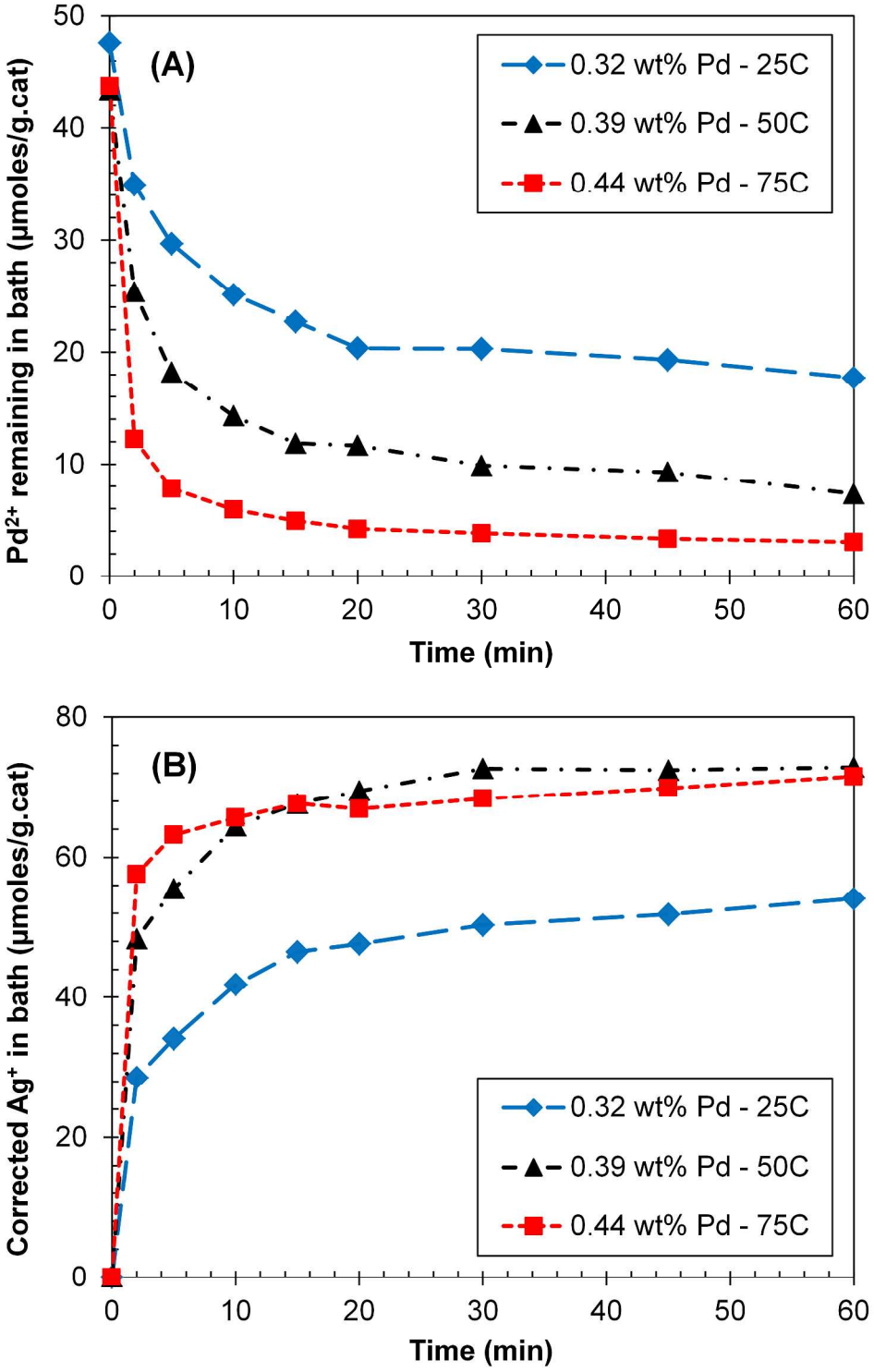

Fig. 3 Time-dependent galvanic displacement profiles of (A) deposited Pd^{2+} from bath solution and (B) galvanically displaced Ag^{+} from 2 wt% Ag/SiO_2 at 25, 50 and 75 °C with same initial Pd^{2+} concentration.

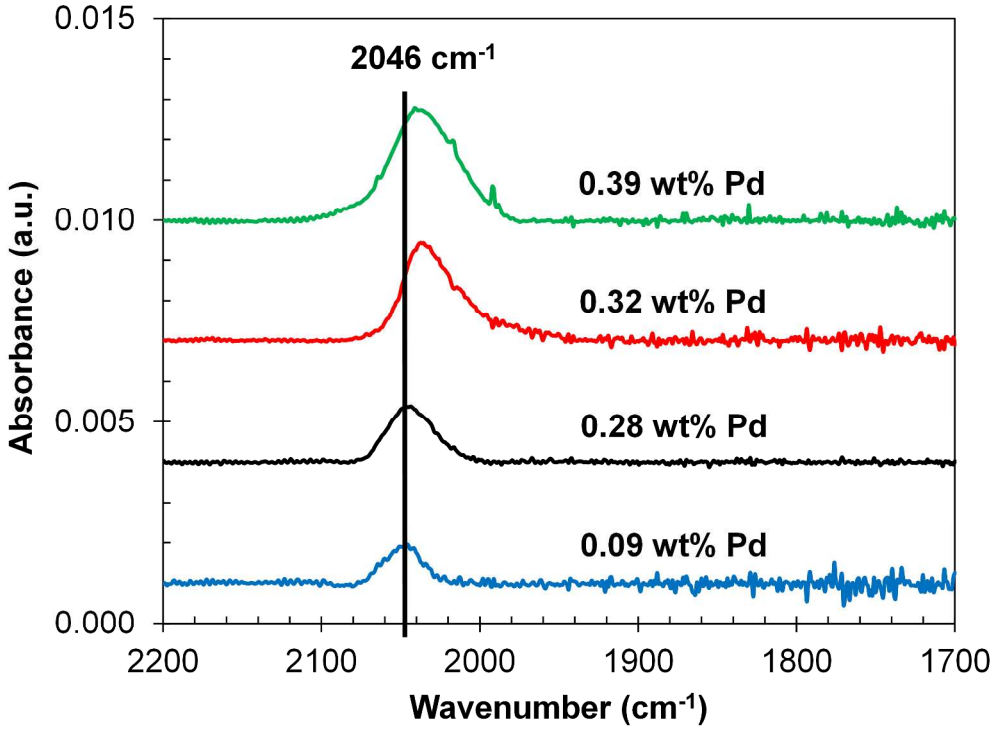

Fig. 4 FTIR spectra for CO adsorption on various Pd-Ag/SiO_2 bimetallic catalysts.

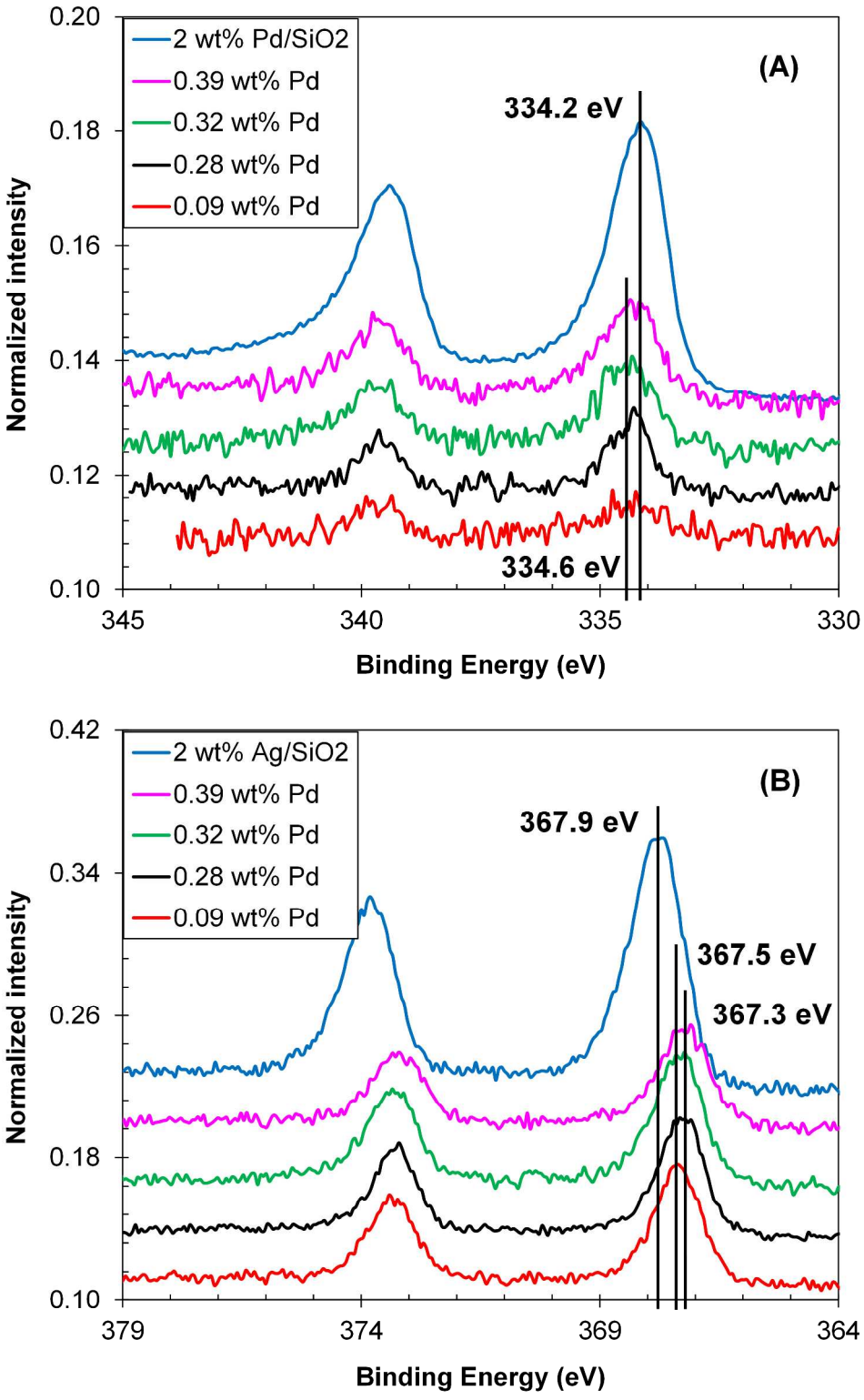

Fig. 5 XPS spectra of (A) Pd 3d on 2 wt% Pd/SiO_2 and $Pd\text{-}Ag/SiO_2$ and (B) Ag 3d on 2 wt% Ag/SiO_2 and $Pd\text{-}Ag/SiO_2$. All samples were reduced *in situ* at 200 °C in 100% H_2 for 2 h.

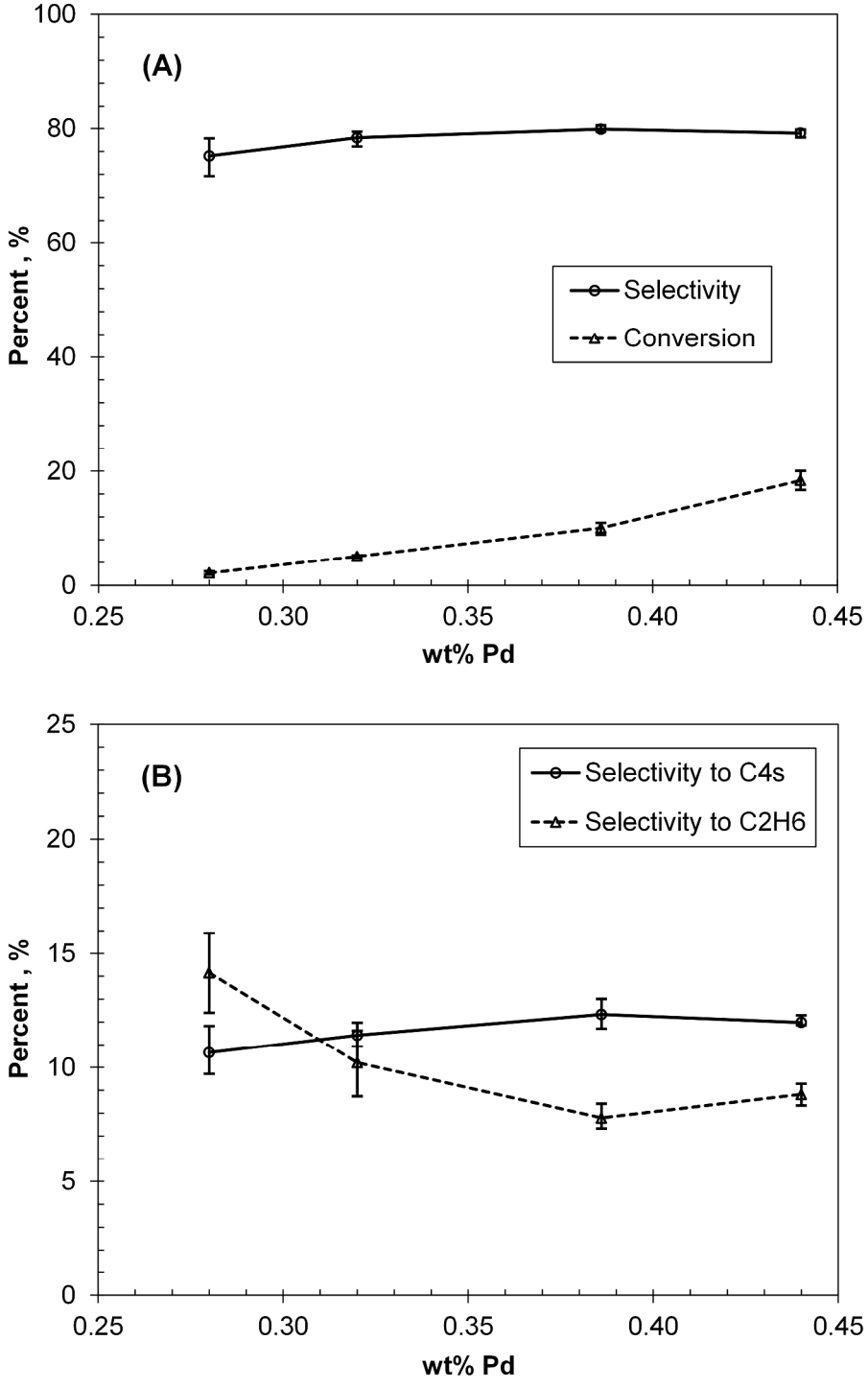

Fig. 6 (A) Conversion of acetylene and selectivity of acetylene to ethylene and (B) selectivity of acetylene to ethane and C_4s as a function of Pd weight loadings on Ag/SiO_2. Reaction conditions: 65°C and feed composition of 1% C_2H_2, 5% H_2, 20% C_2H_4, and balance He at GHSV = 6.0×10^5 h^{-1}. Error bars represent maximum and minimum values for each data point; data point is average value.

Graphical Abstract

Pd-Ag/SiO_2 bimetallic catalysts prepared by galvanic displacement for selective hydrogenation of acetylene in excess ethylene

Yunya Zhang, Weijian Diao, John R. Monnier, and Christopher T. Williams*

Department of Chemical Engineering, University of South Carolina, Swearingen Engineering Center, Columbia, SC 29208, USA. Email: willia84@cec.sc.edu; Tel: +1 (803) 777 0143; Fax: +1 (803) 777 8265

A series of bimetallic Pd-Ag/SiO_2 cataltysts with Ag enriched on the surface were prepared by galvanic displacement. The bimetallic effect for these catalysts on acetylene hydrogenation was discussed.